Near-LTE Linear Response Calculations with a Collisional-Radiative Model for He-like Al Ions

Richard More
Lawrence Livermore National Laboratory, Livermore, California 94550

Takako Kato
National Institute for Fusion Science, Toki, Gifu, 509-52, Japan
(Received 16 January 1998)

This paper establishes a connection between atomic kinetics and nonequilibrium thermodynamics, using a collisional-radiative model modified to include line absorption. Steady-state emission is calculated for He-like aluminum immersed in a specified radiation field having fixed deviations from a Planck spectrum. The calculated net emission is presented as a NLTE response matrix. In agreement with a rigorous general rule of nonequilibrium thermodynamics, the linear response is symmetric. We compute the response matrix for 1% and $\pm 50\%$ changes in the photon temperature and find linear response over a surprisingly large range. [S0031-9007(98)06749-0]

PACS numbers: 52.25.Jm, 05.70.Ln, 52.25.Nr

While radiative properties of dense plasmas such as stellar interiors are usually studied using LTE (local thermodynamic equilibrium) methods, low-density plasmas (tokomak plasmas, the solar corona) require nonequilibrium kinetic models. Intermediate plasmas (laser-produced plasmas, laser hohlraums, pinches, divertor plasmas) combine high density, a significant radiation environment, and non-LTE (NLTE) populations.

This paper examines non-LTE atomic kinetics using methods of nonequilibrium thermodynamics [1–3]. We adapt an existing collisional-radiative (CR) model of Fujimoto and Kato [4] to near-LTE conditions and verify the application of nonequilibrium thermodynamics by finding a symmetric linear-response matrix.

We consider an ion interacting with radiation which is *approximately* a blackbody field at the temperature of the free electrons. The difference between the actual radiation and the blackbody field causes nonequilibrium populations of excited states and leads to a net difference of emission and absorption rates. The difference of emission and absorption at frequency ν is a function of the deviation from the blackbody spectrum at frequency ν' and can be described by a *response matrix* $R_{\nu,\nu'}$.

According to nonequilibrium thermodynamics, the steady state near LTE is constrained by rigorous general requirements of energy conservation, by the principle of minimum entropy production, and by Onsager relations which require that the linear response matrix $R_{\nu,\nu'}$ be symmetric. This symmetry provides a consistency test for a NLTE model.

At high-density, electron collisional rates greatly exceed radiative rates and the deviations from LTE should be small, as shown in previous general studies of NLTE kinetics [5–7]. Recently the effect of radiation on NLTE populations has begun to attract interest [8–11]. In this paper we consider a moderate density and study the effect of coupling to near-equilibrium radiation, which can induce NLTE populations in a controlled manner.

The calculations describe He-like aluminum. The Maxwellian free electrons have a fixed density $N_e = 10^{20}\ \mathrm{cm}^{-3}$ and temperature $T_e = 150$ eV.

The CR model [4] includes 65 He-like levels up to $n = 22$, with $n, 1, S$-splitting up to $n = 4$ and n, S-splitting up to $n = 8$, but does not include autoionizing doubly excited levels. Li-like ions and Li-like satellite levels are omitted.

Electron collisional rates for excitation and de-excitation obey detailed balance. Collisional ionization to and 3-body recombination from the hydrogenlike ion are included. Solution of the collisional-radiative model determines steady-state populations of He-like excited states. The CR model [4] also includes radiative and dielectronic recombination, but for simplicity these have been suppressed.

Because hydrogenlike ions are coupled through collisional ionization and recombination, it is necessary to use the appropriate ratio of heliumlike and hydrogenlike ions. This is done by finding the steady-state solution of the rate equations.

The isotropic radiation field has a spectrum I_ν characterized by the number of photons per mode n_ν. In complete equilibrium, n_ν is the blackbody function,

$$n_\nu^0 = [\exp(h\nu/kT_e) - 1]^{-1}. \tag{1a}$$

Non-LTE populations will be induced by a difference $(n_\nu - n_\nu^0)$. In order to generate the response matrix, a nonequilibrium radiation spectrum is defined by altering n_ν, using

$$n_\nu = [\exp(h\nu/k\{T_e + \delta T_\nu\}) - 1]^{-1}, \tag{1b}$$

where $T_e + \delta T_\nu$ is the effective photon temperature (brightness temperature) for the selected line.

The CR model includes spontaneous emission, described by (dN_i/dt) the rate of radiative transitions $i \rightarrow j$ (i is the upper level, j is the lower level). The initial or final states are also connected to other states (k, l, etc.). We

TABLE I. He-like aluminum transitions.

Transition 1	$1s^2\,{}^1S$–$1s2p\,{}^1P$	1.600 keV
Transition 2	$1s^2\,{}^1S$–$1s3p\,{}^1P$	1.870 keV
Transition 3	$1s2s\,{}^1S$–$1s3p\,{}^1P$	0.276 keV
Transition 4	$1s2p\,{}^1P$–$1s3s\,{}^1S$	0.268 keV
Transition 5	$1s2p\,{}^1P$–$1s3d\,{}^1D$	0.270 keV

now extend the CR model by adding stimulated emission ($A_{ij}N_in_\nu$) and absorption ($A_{ji}N_jn_\nu$) for each transition,

$$(dN_i/dt) = -A_{ij}N_i(n_\nu + 1) + A_{ji}N_jn_\nu + C_i\,. \quad (2)$$

C_i denotes the net collision rate. The absorption coefficient is determined by detailed balance,

$$A_{ji} = (g_i/g_j)A_{ij}\,. \quad (3)$$

Here g_i, g_j are the degeneracies of upper and lower levels. We have verified that, when $n_\nu = n_\nu^0$ for all transitions, the computed population ratios are Boltzmann ratios.

To construct a $k \times k$ response matrix we perform k NLTE calculations. In each, $n_{\nu'}$ is varied for one specific line ν' (Table I) by a photon temperature change $\delta T_{\nu'}$ applied to that line. All other lines still couple to the blackbody spectrum n_ν^0. For each line, in NLTE, there is a net radiated power,

$$dE_{ij}/dt = h\nu[A_{ij}N_i(n_\nu + 1) - A_{ji}N_jn_\nu]\,. \quad (4)$$

This can be positive (emission) or negative (absorption). Equation (4) is zero in LTE (when $n_\nu = n_\nu^0$ and $N_{i,j} = N_{i,j}^0$) and is proportional to $\delta T_{\nu'}$ for small perturbations. In NLTE there is emission or absorption for many lines (see Figs. 1 and 2). The linear response matrix is defined by

$$R_{\nu,\nu'} = h\nu[A_{ij}N_i(n_\nu + 1) - A_{ji}N_jn_\nu]/\delta T_{\nu'}\,. \quad (5)$$

According to nonequilibrium thermodynamics, if $R_{\nu,\nu'}$ is defined in precisely this way, it should be a symmetric matrix.

For large perturbations $\delta T_{\nu'}$, the photon population $n_{\nu'}$ changes strongly, especially for lines with $h\nu' \gg kT_e$. Therefore we examine a modified matrix,

$$\begin{aligned} RL_{\nu,\nu'} &= R_{\nu,\nu'}([\partial n_{\nu'}^0/\partial T]\delta T_{\nu'}/[n_{\nu'} - n_{\nu'}^0]) \\ &= h\nu[A_{ij}N_i(n_\nu + 1) - A_{ji}N_jn_\nu] \\ &\quad \times [\partial n_{\nu'}^0/\partial T]/[n_{\nu'} - n_{\nu'}^0]\,. \end{aligned} \quad (6)$$

The extra factor in Eq. (6) is unity for small perturbations so the modified response matrix is still symmetric in that case. However, $RL_{\nu,\nu'}$ remains constant for larger perturbations.

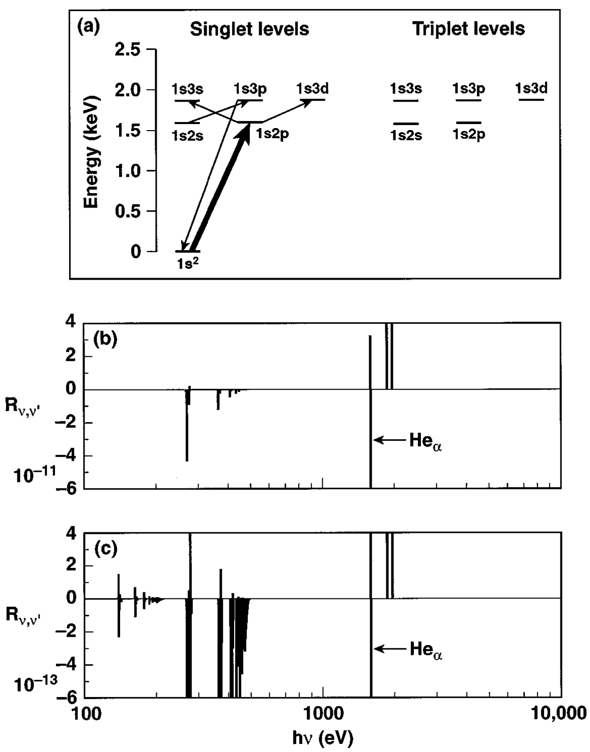

FIG. 1. (a) Basic term diagram for He-like aluminum. When extra radiation is applied to the He$_\alpha$ transition, the $n = 2$ excited states are populated more strongly than in LTE and the $2 \rightarrow 3$ transitions have a net absorption. (b) The response matrix (eV/atom sec) for this case shows absorption (negative R values) for the $2 \rightarrow 3$ transitions. (c) At higher magnification, many other transitions show small responses. The plasma conditions are given in Tables II, IIIa, and IIIb.

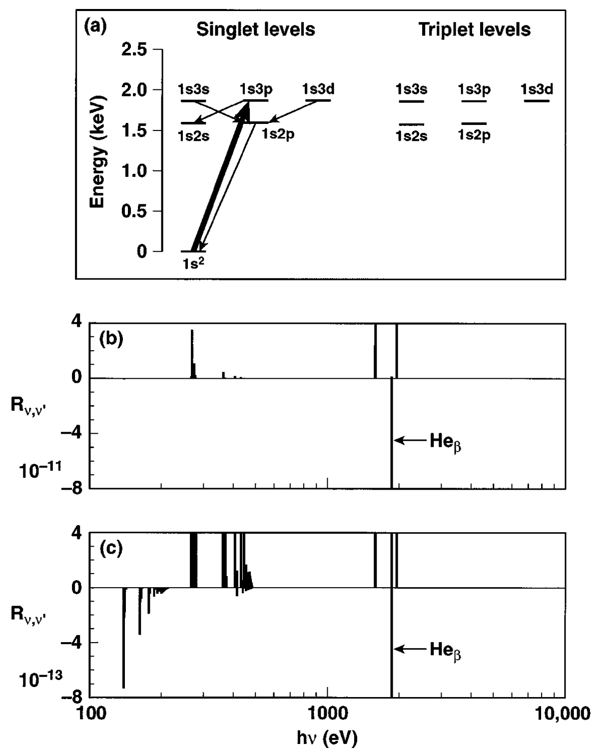

FIG. 2. (a) In this case, the perturbation is applied to the He$_\beta$ transition. Now the $2 \rightarrow 3$ transitions have net emission, as does the He$_\alpha$ line. (b) The signs of $2 \rightarrow 3$ response coefficients at 280 eV have become positive. (c) At higher magnification, many other transitions show small responses.

TABLE II. Linear-response coefficients (W/atom eV) for He-like aluminum plasma at electron density $n_e = 10^{20}$ cm^{-3} and temperature $T_e = 150$ eV. The matrix is obtained by averaging NLTE calculations with $+1\%$ and -1% perturbations in lines identified in Table I. The matrix is nearly symmetric.

	1	2	3	4	5
1	-5.234×10^{-10}	3.564×10^{-10}	-9.317×10^{-12}	-1.662×10^{-12}	-4.333×10^{-11}
2	3.564×10^{-10}	-6.221×10^{-10}	1.068×10^{-11}	1.590×10^{-12}	3.538×10^{-11}
3	-9.317×10^{-12}	1.068×10^{-11}	-2.344×10^{-12}	1.178×10^{-14}	2.449×10^{-13}
4	-1.662×10^{-12}	1.590×10^{-12}	1.177×10^{-14}	-3.601×10^{-13}	4.507×10^{-14}
5	-4.333×10^{-11}	3.538×10^{-11}	2.449×10^{-13}	4.506×10^{-14}	-8.827×10^{-12}

Table I labels the transitions studied in Tables II, IIIa, and IIIb. The transitions are in the singlet spectrum but the calculation includes coupling to triplet states. Table II gives the linear-response matrix calculated as the average of $RL_{\nu,\nu'}$ for small radiation temperature changes of $+1\%$ and -1%. Tables IIIa and IIIb give $RL_{\nu,\nu'}$ for temperature perturbations of $\pm 50\%$.

The linear-response matrix in Table II is accurately symmetric. Tables IIIa and IIIb indicate the range of linear response. For the He$_\beta$ transition, a 50% increase in photon temperature raises the photon flux by a factor of 60, while a 50% decrease reduces n_ν by a factor of 10^{-5}. The range of linear response is surprisingly large.

However, these perturbations affect only one line and we expect nonlinear response for sufficiently strong perturbations affecting several lines.

To interpret the response function, we consider a perturbation of the He$_\alpha$ line (see Fig. 1 and Table II). In this case, $n_{\nu'}$ is increased relative to $n^0_{\nu'}$ for absorption from the $1s^2$ ground state to the $1s2p\,^1P$ excited state, and this produces a negative diagonal matrix element. The absorption decreases the ground state population and increases the $(1s2p\,^1P)$ population.

Since the ground state population is reduced, there is net emission for the line $1s3p\,^1P \rightarrow 1s^2$. Because the population of $1s2p\,^1P$ is higher than LTE, there is net absorption for transitions $1s2p\,^1P \rightarrow 1s3s\,^1S$ and $1s2p\,^1P \rightarrow 1s3d\,^1D$. There is enough collisional transfer $1s2p\,^1P \rightarrow 1s2s\,^1S$ to overpopulate $1s2s\,^1S$ and for that reason there is also weak absorption for $1s2s\,^1S \rightarrow 1s3p\,^1P$. From Fig. 1 it is seen that the $(1s2p\,^3P - 1s^2\,^1S)$ intercombination line has net emission, and the transitions from $n = 4$ to $n = 2$ are absorptions. At higher magnification many weak emitting and absorbing transitions are seen [Fig. 1(c)].

When the radiation is enhanced in the He$_\beta$ ($1s^2\,^1S \rightarrow 1s3p\,^1P$) line, the ground state population is reduced and $1s3p\,^1P$ is raised relative to LTE (Fig. 2). The second row of the response matrix in Table II has all signs reversed. There is weak emission for $3 \rightarrow 2$ transitions, principally because of collisional transfer between the $n = 3$ levels which distributes the enhanced population of the $1s3p\,^1P$ state. The $1s2p\,^1P$ population increases by cascade and there is net emission on the resonance transition $(1s2p\,^1P \rightarrow 1s^2\,^1S)$. The rest of the matrix is easily understood by similar reasoning.

We have performed calculations (described elsewhere) for the same density-temperature conditions using a NLTE screened-hydrogenic average-atom model [12], which gives qualitatively similar results for the response

TABLE IIIa. Response coefficient $\mathrm{RL}_{u,v}$ (W/atom eV) for He-like aluminum plasma at electron density $n_e = 10^{20}$ cm^{-3}, temperature $T_e = 150$ eV. The perturbations are 50% of Te.

	1	2	3	4	5
1	-5.230×10^{-10}	3.561×10^{-10}	-9.309×10^{-12}	-1.661×10^{-12}	-4.329×10^{-11}
2	3.563×10^{-10}	-6.220×10^{-10}	1.068×10^{-11}	1.589×10^{-12}	3.537×10^{-11}
3	-7.335×10^{-12}	8.407×10^{-12}	-1.845×10^{-12}	9.269×10^{-15}	1.928×10^{-13}
4	-1.651×10^{-12}	1.579×10^{-12}	1.170×10^{-14}	-3.577×10^{-13}	4.477×10^{-14}
5	-3.993×10^{-11}	3.260×10^{-11}	2.257×10^{-13}	4.153×10^{-14}	-8.135×10^{-12}

TABLE IIIb. Response coefficient $\mathrm{RL}_{u,v}$ (W/atom eV) for He-like aluminum plasma at electron density $n_e = 10^{20}$ cm^{-3} and temperature $T_e = 150$ eV. The perturbation is -50% of Te; as emphasized in the text, a large perturbation.

	1	2	3	4	5
1	-5.234×10^{-10}	3.564×10^{-10}	-9.317×10^{-12}	-1.662×10^{-12}	-4.333×10^{-11}
2	3.564×10^{-10}	-6.222×10^{-10}	1.068×10^{-11}	1.590×10^{-12}	3.538×10^{-11}
3	-1.156×10^{-11}	1.326×10^{-11}	-2.908×10^{-12}	1.461×10^{-14}	3.040×10^{-13}
4	-1.670×10^{-12}	1.597×10^{-12}	1.183×10^{-14}	-3.618×10^{-13}	4.528×10^{-14}
5	-4.619×10^{-11}	3.772×10^{-11}	2.611×10^{-13}	4.804×10^{-14}	-9.410×10^{-12}

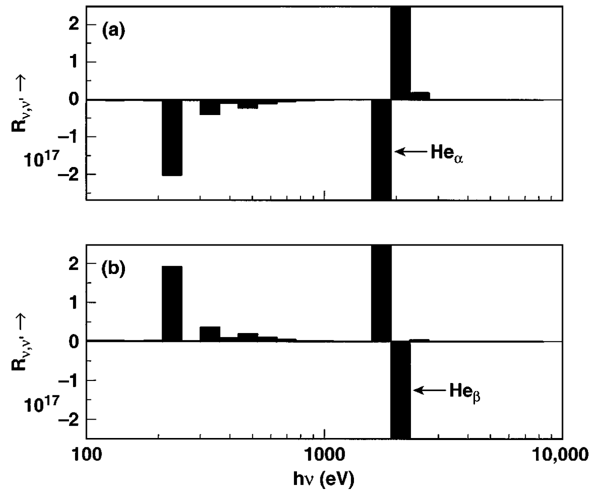

FIG. 3. Calculations from the NLTE screened-hydrogenic average-atom model for aluminum plasma at the conditions described in Table II. The response matrix, shown here as a histogram, is normalized by frequency group widths for emitting and perturbed portions of the radiation spectrum and has units of $W/g\,keV^3$. For perturbation of He_α (a) and He_β (b) lines, the signs of the response coefficients agree with results from the CR model.

matrix (see Fig. 3). In this case, the response function is averaged over frequency groups for perturbed and emitting parts of the spectrum, and has units of $W/g\,keV^3$. With appropriate conversion of units the numerical values approximately agree with the CR model.

This agreement is interesting because the average-atom model does not have singlet-triplet splitting but includes photoionization, radiative recombination, and an approximate treatment of other ion charge states.

The work described in this paper could be extended in several directions. If one examined response within the Doppler profile, the ion temperature would enter the discussion. If the electron distribution were slightly non-Maxwellian, there would be an analogous response function defining response to perturbations of the electron distribution. In addition, there are questions about non-linear response and the combination of the rate-equation description with more fundamental theory of multiphoton processes.

The linear-response method considered here is limited to a special class of NLTE states. The system must be in a steady state and must be "near" LTE, although in these calculations we have found a large range of linear response. We believe this response function can be used to simplify the calculation of NLTE atomic kinetics in plasma simulation calculations.

Professor Hans Griem made helpful comments on a draft version of this manuscript, and Dr. S. Libby, Dr. F. Graziani, and Dr. G. Zimmerman have contributed useful ideas and suggestions. J. Levatin assisted with the numerical calculations. This work was supported in part under the auspices of the U.S. Department of Energy by Lawrence Livermore National Laboratory under Contract No. W-7405-ENG-48 and the US-Japan Fusion Cooperation Program.

[1] R. More, p. 399 in *Atomic and Molecular Physics of Controlled Thermonuclear Fusion*, edited by C. Joachain and D. Post (Plenum, New York, 1983).
[2] S. Libby, F. Graziani, R. More, and T. Kato, in *Proceedings of the 13th International Conference on Laser Interactions and Related Plasma Phenomena*, edited by G. Miley and E. Campbell (AIP, New York, 1997).
[3] I. Prigogine, *Thermodynamics of Irreversible Processes* (Interscience, New York, 1967), 3rd ed.; K. Denbigh, *Thermodynamics of the Steady State* (Methuen, London, 1965).
[4] T. Fujimoto and T. Kato, Nagoya University Institute of Plasma Physics Report No. IPPJ-647, 1983 (unpublished); Phys. Rev. A **30**, 379 (1984); Phys. Rev. A **32**, 1663 (1985); Phys. Rev. A **35**, 3024 (1987)
[5] M. Klapisch, J. Phys. (Paris), Colloq. Suppl. C1 **3**, 49 (1988).
[6] D. Salzmann, Phys. Rev. A **20**, 1704 (1979); Phys. Rev. A **20**, 1713 (1979); Phys. Rev. A **21**, 1761 (1980).
[7] T. Fujimoto, J. Phys. Soc. Jpn. **47**, 265 (1979); **47**, 273 (1979); **49**, 1561 (1980); **49**, 1569 (1980); **54**, 2905 (1985).
[8] J. Abdallah, Jr., R. Clark, C. Keane, T. Shepard, and L. Suter, J. Quant. Spectrosc. Radiat. Transf. **50**, 91 (1993).
[9] M. Busquet, J. Quant. Spectrosc. Radiat. Transf. **58**, 519 (1997); M. Busquet, Phys. Fluid B **5**, 4191 (1993).
[10] S. J. Rose, J. Quant. Spectrosc. Radiat. Transf. **54**, 333 (1995).
[11] H. Griem, *Principles of Plasma Spectroscopy* (Cambridge University Press, Cambridge, England, 1997).
[12] D. E. Post *et al.*, At. Data Nucl. Tables **20**, 397 (1977); G. B. Zimmerman and R. M. More, J. Quant. Spectrosc. Radiat. Transf. **23**, 517 (1980); R. More, J. Quant. Spectrosc. Radiat. Transf. **27**, 345 (1982).